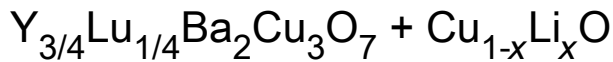


Superconductor-semiconductor-super-conductor junction network in bulk polycrystalline composites



To cite this article: M I Petrov *et al* 2001 *Supercond. Sci. Technol.* **14** 798

View the [article online](#) for updates and enhancements.

Related content

- [Magneto-resistive effect in bulk composites 1-2-3 YBCO + CuO and 1-2-3 YBCO + BaPb_xSn_{1-x}O₃ and their application as magnetic field sensors at 77 K](#)
D A Balaev, K A Shaikhutdinov, S I Popkov *et al.*
- [Study of dependence upon the magnetic field and transport current of the magneto-resistive effect in YBCO-based bulk composites](#)
D A Balaev, A G Prus, K A Shaykhutdinov *et al.*
- [A dc superconducting fault current limiter using die-pressed YBa₂Cu₃O₇ ceramic](#)
A G Mamalis, M I Petrov, D A Balaev *et al.*

Recent citations

- [New Evidence of Interaction Between Grain and Boundaries Subsystems in Granular High-Temperature Superconductors](#)
D. A. Balaev *et al*
- [Nonmonotonic behavior of magneto-resistance, R\(H\) hysteresis, and low-temperature heat capacity of the BaPb_{0.75}Bi_{0.25}O₃ superconductor in a magnetic field: Possible manifestations of phase separation](#)
D. A. Balaev *et al*
- [Magneto-resistance hysteresis in granular HTSCs as a manifestation of the magnetic flux trapped by superconducting grains in YBCO + CuO composites](#)
K. A. Shaikhutdinov *et al*



IOP | ebooks™

Bringing together innovative digital publishing with leading authors from the global scientific community.

Start exploring the collection—download the first chapter of every title for free.

Superconductor–semiconductor–superconductor junction network in bulk polycrystalline composites

$\text{Y}_{3/4}\text{Lu}_{1/4}\text{Ba}_2\text{Cu}_3\text{O}_7 + \text{Cu}_{1-x}\text{Li}_x\text{O}$

M I Petrov, D A Balaev, K A Shaihtudinov and K S Aleksandrov

Kirensky Institute of Physics, 660036 Krasnoyarsk, Russia

Received 23 July 2001

Published 22 August 2001

Online at stacks.iop.org/SUST/14/798

Abstract

Bulk $\text{Y}_{3/4}\text{Lu}_{1/4}\text{Ba}_2\text{Cu}_3\text{O}_7 + \text{Cu}_{1-x}\text{Li}_x\text{O}$ composites with $x = 0, 0.003$ and 0.06 and varied volume content of $\text{Cu}_{1-x}\text{Li}_x\text{O}$ have been prepared. Analysis of the transport properties of the composites has shown that they can be represented as a network of superconductor–semiconductor–superconductor (S–Sm–S) weak links. The dependence of the critical current density on the normal resistance for the composites studied shows a behaviour similar to that for single Josephson junctions. The experimental temperature dependences of the critical current are qualitatively described in terms of a theory of S–Sm–S junctions that takes into account the Andreev reflection of carriers from the S–Sm and Sm–S interfaces.

1. Introduction

The transport properties of polycrystalline high-temperature superconductors (HTSC) are affected by native grain boundaries forming weak links between the superconductor crystallites [1–2]. In HTSC-based composites, the non-superconducting material (normal metal (N) [3–14] or insulator (I) [15–20]) plays the role of artificially created grain boundaries. HTSC-based composites are of considerable interest not only because of their possible practical applications, but also as objects for studying intergrain coupling [5, 7–9, 14, 17, 19, 20]. Analysis of the transport properties of the composites in terms of the various models developed for Josephson junctions should indicate applicability (or inapplicability) of these models to HTSC. Experimental works are presently focused on HTSC + normal metal [3–14] or HTSC + insulator [15–20] composites. Superconductor–semiconductor–superconductor (S–Sm–S) junctions are weak links with intermediate properties between that of tunnel and S–N–S junctions. Therefore, an experimental study of HTSC + semiconductor composites would be advisable.

In a previous study [20], we demonstrated that HTSC + CuO composites prepared by the fast baking method can be considered as a model of network S–I–S junctions. Non-isovalent impurity doping of CuO with $\text{Li} \rightarrow \text{Cu}$ makes

the carrier concentration in CuO higher [21]. It seems natural to assume, therefore, that an S–Sm–S network of weak links will be realized in HTSC + $\text{Cu}_{1-x}\text{Li}_x\text{O}$ composites.

A composite is a typical example of a Josephson network characterized by some grain boundary thickness distribution depending on the volume content of ingredients and on the preparation technique. Analyses of the transport properties of composites prepared by the method of fast baking [13, 14, 20] have shown, however, that a composite may be described by some effective grain boundary thickness. Its current–voltage characteristics and temperature dependences of the critical current density and resistivity show basic features of single Josephson junctions. Making the baking time shorter leads to a shift and broadening of the superconductor–non-superconductor percolation threshold to lower non-superconductor content in contrast to composites prepared by prolonged heat treatment. In the case of fast baking, the transport current flows through both superconductor and non-superconductor grains at relatively small concentrations (7–45 vol%) of the latter ingredient [19, 20]. Therefore, the effective thickness of layers between superconductor crystallites can be easily changed by varying the relative volume content of components of a composite [13, 20].

In the present study, we prepared HTSC + $\text{Cu}_{1-x}\text{Li}_x\text{O}$ composites with $x = (0–0.06)$ and $\text{Cu}_{1-x}\text{Li}_x\text{O}$ volume

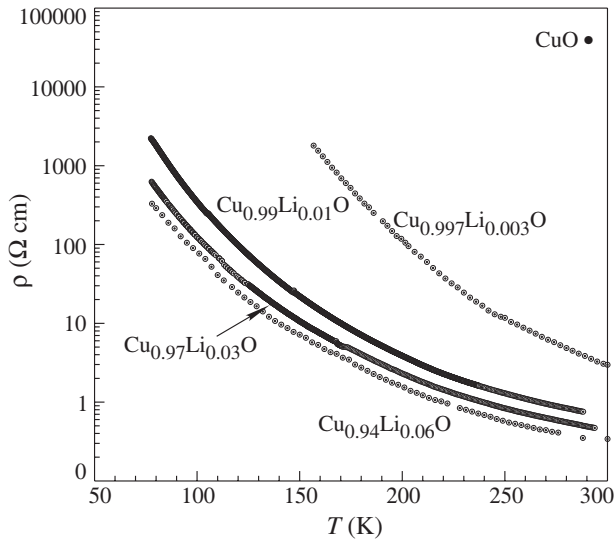


Figure 1. Temperature dependences of the resistivity of $\text{Cu}_{1-x}\text{Li}_x\text{O}$ compounds.

content in the range 0–30%. The effect exerted by the increase in the semiconductor carrier concentration on the resistivity, critical current density and current–voltage characteristics of the composites is discussed in terms of models developed for S–Sm–S Josephson junctions. In addition, the relevant published data being contradictory [21–23], we analysed the temperature behaviour of $\text{Cu}_{1-x}\text{Li}_x\text{O}$ resistivity and magnetization.

2. Experimental methods

The electrical resistivity of $\text{Cu}_{1-x}\text{Li}_x\text{O}$ compounds was measured by dc four-probe (low resistivity case) and two-probe (high resistivity) techniques in constant-current and constant-voltage modes, respectively. The constant current (or voltage) was chosen within the range where Ohm’s law is obeyed. The data obtained in these two modes coincided.

The $\rho(T)$ dependences were measured for the composites by the standard four-probe technique. For measurements below T_C , the current was $0.01 \times J_C(4.2 \text{ K})$, ($J_C(4.2 \text{ K})$ is the critical current density at 4.2 K). In this case, lowering the current had no effect on the $\rho(T)$ dependences and the ‘zero-resistivity’ ($\rho \approx 10^{-6} \Omega \text{ cm}$) temperature.

The current–voltage (I – V) characteristics of the composites were measured using the standard four-probe technique. The current contact pads were coated with a layer of In–Ga eutectics. The area of the current contact pads was about two orders of magnitude larger than the cross-sectional area of the ‘working’ part of the sample ($1 \times 0.2 \text{ mm}^2$), see figure 1 in [24]. The sample was glued onto a sapphire substrate attached to a silver rod. The critical current J_C was determined from the initial portion of I – V characteristics, using the standard criterion $1 \mu\text{V cm}^{-1}$ [25]. In order to measure I – V characteristics at high current densities $j \gg J_C$, the cell with a sample was placed on a liquid helium bath. The I – V characteristics presented in this communication were measured under constant-current conditions and were fully reproducible at any current sweep rate. This ensured that no self-heating effects

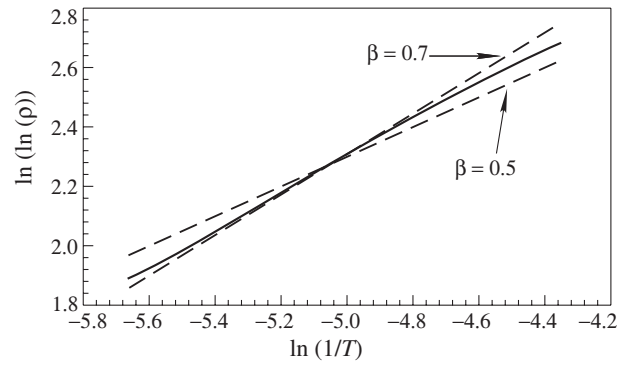


Figure 2. The log–log plot of the resistivity ρ of $\text{Cu}_{0.99}\text{Li}_{0.01}\text{O}$ versus $1/T$ (full curve). The broken curves represent fits with equation (1). The least-squares fit gives a value $\beta = 0.6$.

occurred. Magnetic measurements were performed using a vibration sample magnetometer.

3. Results and discussion

3.1. Preparation and physical properties of $\text{Cu}_{1-x}\text{Li}_x\text{O}$ compounds

The semiconductor components of the composites were synthesized from CuO and Li_2CO_3 , according to the following scheme. The powders were thoroughly mixed, compacted into pellets and calcined in air at 700°C during 10 h. Then the resulting product was milled in an agate mortar, compacted into pellets and calcined at 800°C for 1 h. Using this scheme, we prepared $\text{Cu}_{1-x}\text{Li}_x\text{O}$ samples with $x = 0, 0.003, 0.01, 0.03$ and 0.06 . According to [23], the solubility limit of lithium in copper is in the range 4–10 at.%. For this reason, no samples with $x > 0.06$ were prepared.

X-ray diffraction (XRD) patterns of a $\text{Cu}_{0.94}\text{Li}_{0.06}\text{O}$ sample with the highest Li content shows only reflections from the CuO phase, corresponding to the same cell parameters as those in pure CuO .

Figure 1 shows a semi-logarithmic plot of resistivity versus temperature for $\text{Cu}_{1-x}\text{Li}_x\text{O}$ samples. The steady decrease in resistance with increasing x can be seen over a wide temperature range. We fitted the experimental $\rho(T)$ dependences using the expression:

$$\rho(T) \sim \exp(T^{-\beta}). \quad (1)$$

Figure 2 presents an example of how the experimental exponent β was determined for a $\text{Cu}_{0.99}\text{Li}_{0.01}\text{O}$ sample. It can be seen that the dependence of $\ln(\ln \rho)$ on $\ln(1/T)$ shows a variety of slopes in different temperature ranges and, correspondingly, is characterized by a variety of exponents in equation (1) (0.5 to 0.7). Similar kinks in the $\ln \rho(1/T)$ dependence have been observed on single crystals and polycrystalline $\text{Cu}_{1-x}\text{Li}_x\text{O}$ samples [22, 23]. The kinks seem to correspond to antiferromagnetic transitions [22]. Table 1 lists experimental exponents β and other parameters of the $\text{Cu}_{1-x}\text{Li}_x\text{O}$ samples studied. For a sample with relatively low Li concentration, $\text{Cu}_{0.997}\text{Li}_{0.003}\text{O}$, the conventional thermal resistivity mechanism takes place ($\beta \approx 1$, similarly to CuO without Li [22]). Raising the content of lithium

Table 1. Some parameters of $\text{Cu}_{1-x}\text{Li}_x\text{O}$ compounds. The activation energy E_g is calculated with thermally activated process ($\ln \rho \sim 1/T$) in a high temperature range above the Neel temperature. β is the experimental exponent in equation (1). T_N is the Neel temperature determined from magnetic measurements. N is the carrier concentration calculated in assumption of every lithium ion induces one hole carrier.

| x | $\rho(270\text{ K})$ ($\Omega\text{ cm}$) | E_g (meV) | β | T_N (K) | N (cm^{-3}) |
|-------|--|-------------------|------------------|---------------|-----------------------------|
| 0 | 6×10^4 | 1350 ^a | 1.0 ^a | 230 ± 0.5 | |
| 0.003 | 6.20 | 92 | 0.9 ± 0.05 | 225 ± 0.5 | 1.5×10^{20} |
| 0.01 | 0.94 | 46 | 0.6 ± 0.1 | 223 ± 0.5 | 5.0×10^{20} |
| 0.03 | 0.63 | 43 | 0.6 ± 0.1 | 222 ± 0.5 | 1.5×10^{21} |
| 0.06 | 0.44 | 43 | 0.6 ± 0.1 | 220 ± 1.0 | 3.0×10^{21} |

^aData from [22]

in CuO results in the β value changing to 0.6, which is close to $\beta = 0.5$, predicted theoretically for a doped crystalline semiconductor [26]. It is important to note that an exponent $\beta \approx 0.25$ has been observed for polycrystalline $\text{Cu}_{1-x}\text{Li}_x\text{O}$ [23] and the data obtained have been analysed in terms of the variable-range hopping mechanism. The possible reason for this disagreement may be that different ways of preparations have been used.

The activation energies E_g determined from $\rho(T)$ in the high-temperature range above the Neel temperature with thermally activated process ($\ln \rho \sim 1/T$) listed in table 1 decrease with increasing Li content. This behaviour is in good agreement with the data reported in [23].

The carrier concentration n (see table 1) was calculated on the assumption that each lithium ion gives rise to one hole. In [21], polycrystalline $\text{Cu}_{0.98}\text{Li}_{0.02}\text{O}$ was studied and carrier concentration $n = 4 \times 10^{18}\text{ cm}^{-3}$ was determined from the Hall-effect measurements. This value is 3 orders of magnitude lower than the estimated carrier concentrations in table 1. This discrepancy seems to be due to the high volatility of lithium in synthesis. The lithium vapour pressure at $T = 1000^\circ\text{C}$ (sintering temperature of $\text{Cu}_{0.98}\text{Li}_{0.02}\text{O}$ in [21]) is ~ 50 Torr [27]; for this reason we chose a sintering temperature of $700\text{--}800^\circ\text{C}$, at which the lithium vapour pressure is 1–5 Torr [27].

CuO is known to be an antiferromagnetic with Neel temperature $T_N \approx 30\text{ K}$ [22, 23]. Lithium incorporation into CuO makes the T_N lower [28]. Temperature dependences of magnetization of our $\text{Cu}_{1-x}\text{Li}_x\text{O}$ samples, measured at applied field of 2 kOe, confirmed this effect (see table 1).

Thus, we synthesized $\text{Cu}_{1-x}\text{Li}_x\text{O}$ compounds and measured the temperature dependences of their resistivity and magnetization. The results obtained indicate that lithium dissolves in the CuO matrix.

3.2. Preparation, phase composition and critical temperatures of the composites

The composites were prepared as follows. The HTSC ($\text{Y}_{3/4}\text{Lu}_{1/4}\text{Ba}_2\text{Cu}_3\text{O}_7$) was synthesized using a standard procedure. The components of a composite were thoroughly mixed with additional milling of the powders in an agate mortar and then compacted into pellets. The pellets were placed in preheated boats and then placed in a furnace heated to 900°C . The pellets were kept at this temperature for 2 min and then placed in another furnace for 2.5 h at 350°C , which was followed by furnace-cooling to room temperature.

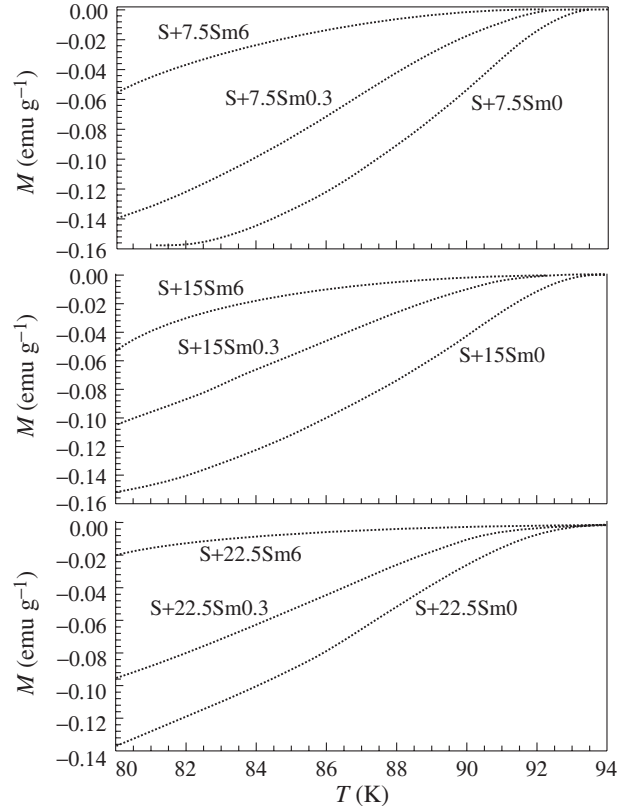


Figure 3. Temperature dependences of dc zero-field-cooled magnetization of the composites.

All composite samples were prepared simultaneously and from the same batches of starting components to minimize variations in the physical properties of the composites, related to stoichiometry and the preparation technique. The resistivities and critical current densities of samples of the same composition varied by less than 10%. A bench-mark sample without $\text{Cu}_{1-x}\text{Li}_x\text{O}$ addition, subjected to the same milling and thermal treatment as the composites, had superconducting properties common for (optimally oxygen-doped) HTSC with 1–2–3 structure ($T_C = 93.5\text{ K}$, $T_C(R = 0) = 91.2\text{ K}$, $J_C(4.2\text{ K}) = 1400\text{ A cm}^{-2}$ [13]). Henceforth we designate the samples as S + VSmX, where V is the volume content of the semiconductor (Sm) component in a composite, X is the atomic percentage of Li in CuO (i. e. Sm0 is CuO, Sm0.3 is $\text{Cu}_{0.997}\text{Li}_{0.003}\text{O}$ etc).

XRD patterns of the composites S + 22.5Sm0, S + 22.5Sm0.3, and S + 22.5Sm6 show only reflections from

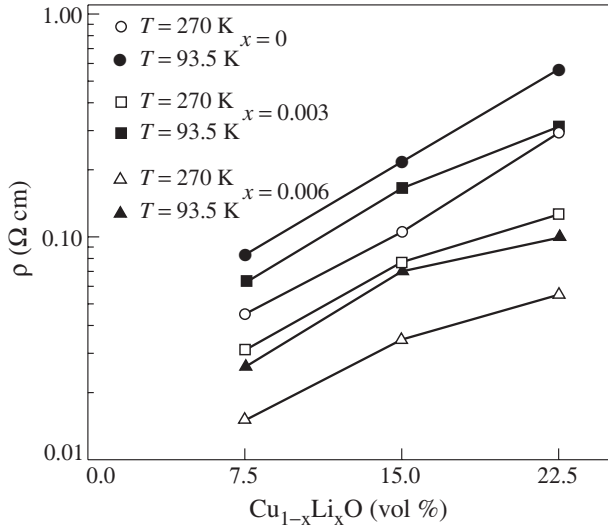


Figure 4. Variation of normal-state (270 K and 93.5 K) resistivity ρ of the composites with volume percentage of $\text{Cu}_{1-x}\text{Li}_x\text{O}$.

HTSC with 1–2–3 structure and CuO. No additional reflections were detected. This indicates the absence (to within XRD accuracy) of any strong chemical reaction between HTSC and $\text{Cu}_{1-x}\text{Li}_x\text{O}$ that could result in the appearance of foreign phases.

Figure 3 shows temperature dependences of magnetization of composite samples, measured in a field of 33 Oe. It is seen that the absolute values of magnetization decrease with increasing Li content in the semiconductor component. The strongest T_C depression observed for sample S + 22.5Sm6 (composite with the highest Li content) is equal to ~ 2.5 K; $T_C \approx 91$ K. This non-dramatic reduction of the superconductivity of HTSC crystallites on raising the Li content in CuO reflects the well known fact of T_C lowering upon doping HTSC having 1–2–3 structure with alkali cations [29] and arises from Li diffusion into the superconductor during baking, even if this time is extremely short (2 min). This lowering of T_C (1–2 K) is insignificant, however, as compared with the T_C of the starting HTSC (93.5 K).

3.3. Temperature dependences of the resistivity of the composites in normal state

The $\rho(300\text{ K})$ and $\rho(93.5\text{ K})$ of the composites increase on both raising the volume content of the semiconductor and decreasing the Li concentration in $\text{Cu}_{1-x}\text{Li}_x\text{O}$, see figure 4. Above T_C , the $\rho(T)$ dependences of the composites exhibit semiconductor-like behaviour shown in figure 5 for samples S + 22.5Sm6 and S + 22.5Sm0.3. It should be noted that HTSC + insulator composites with insulator volume content of up to $\sim 60\%$, prepared by prolonged heat treatment (> 10 h), usually show metal-like or temperature-independent $\rho(T)$ dependences above T_C [16, 17]. This fact is due to the formation of a continuous superconducting cluster during prolonged preparation. Extremely short baking seems to fuse composite component particles (whose size of $\sim 1\ \mu\text{m}$ is determined by grinding) without crystallite growth occurring in the case mentioned above. In order to compare our data with the results of other groups we extended the high-temperature

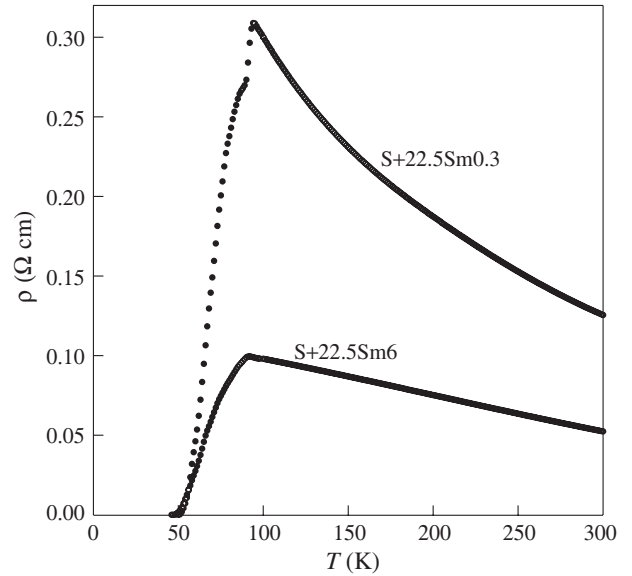


Figure 5. Temperature dependences of the resistivity ρ of composite samples S + 22.5Sm0.3 and S + 22.5Sm6.

baking time of composites S + VSm0 to 1 h. This changed the $\rho(T)$ behaviour to metallic-like for samples with CuO volume content of up to 50% (the details of this study can be found elsewhere).

Thus, in the HTSC + $\text{Cu}_{1-x}\text{Li}_x\text{O}$ composites prepared by fast baking the transport current flows through both the HTSC and the semiconductor grains.

3.4. Temperature dependences of resistivity of the composites below T_C

A sharp drop in resistivity at $T_C \approx 92$ K for sample S + 22.5Sm0.3 (figure 5) is caused by the superconducting transition in the HTSC crystallites and coincides with the T_C determined from magnetic measurements (see figure 3). For sample S + 22.5Sm6 the transition is slightly broadened, which may result from the deterioration of the superconducting properties of HTSC crystallites, caused by lithium diffusion into HTSC [29] (see section 3.2). The zero resistivity temperature of the composites depends on the volume content of the semiconductor and its conductivity. This temperature grows with increasing lithium concentration in $\text{Cu}_{1-x}\text{Li}_x\text{O}$ (i.e. with increasing ρ of $\text{Cu}_{1-x}\text{Li}_x\text{O}$, see figure 1) and decreases with increasing $\text{Cu}_{1-x}\text{Li}_x\text{O}$ volume content.

A broad-foot structure of the $\rho(T)$ dependences below T_C comes from the transition of the network of weak links [13, 20]. A similar $\rho(T)$ behaviour has been observed in polycrystalline HTSC [30–32] and single HTSC weak links [33] and has been interpreted in terms of models developed for Josephson junctions. In [20], we demonstrated that this part of the $R(T)$ dependence of composites HTSC + CuO is excellently described by the mechanism of thermally-activated phase slippage (TAPS) [34]. Therefore, it is reasonable to treat experimental $R(T)$ dependences for HTSC + $\text{Cu}_{1-x}\text{Li}_x\text{O}$ composites within the TAPS approach.

In the limit of a very small transport current, the theory [34]

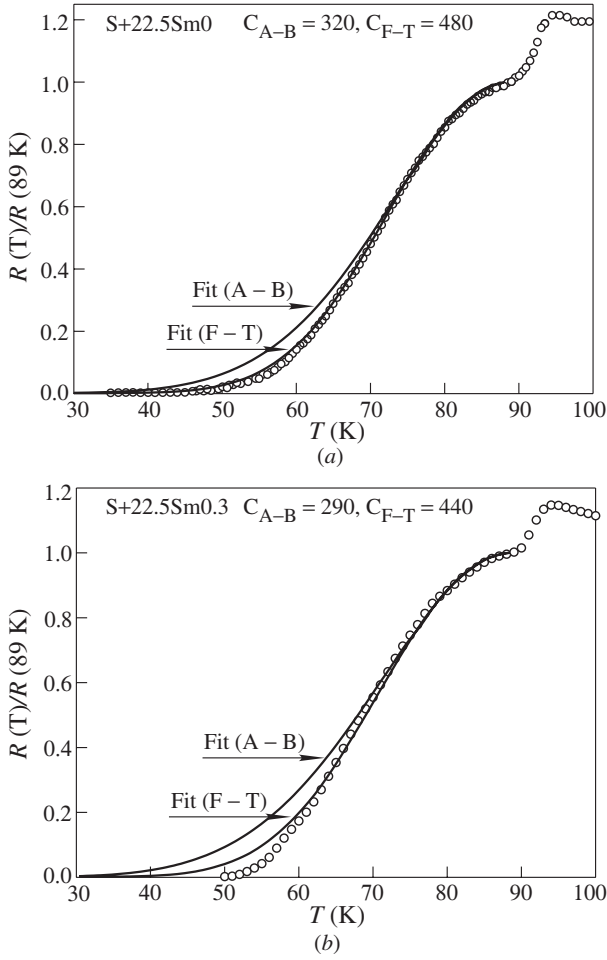


Figure 6. Experimental temperature dependences of the normalized resistivity of composite samples (a) S + 22.5Sm0 and (b) S + 22.5Sm0.3. Full curves are computed by means of equation (2) from the Ambegaokar–Baratoff [35] and Furusaki–Tsukada [36] temperature dependences of the critical current as $I_1(T)$ and the corresponding fitting parameters C_{A-B} and C_{F-T} shown in the figure, $T_C = 89$ K.

predicts that the resistance R_P caused by TAPS is given by

$$\frac{R_P}{R} = \left[I_0 \left(\frac{C I_1(T)}{T} \right) \right]^{-2} \quad (2)$$

where I_0 is a modified Bessel function, $I_1(T)$ is the critical current without fluctuation, and C is the fitting parameter determined in [33].

In figure 6, the normalized resistive transition $R(T)/R(89\text{ K})$ in the S + 22.5Sm x composites is plotted together with the R_P/R dependences calculated by means of equation (2), using C as the fitting parameter and the temperature dependences of the critical current for the S–I–S Josephson junction of Ambegaokar–Baratoff (AB) [35] and Furusaki–Tsukada (FT) [36], as $I_1(T)$. The FT dependence was obtained by the authors for a S–I–S junction with finite I-layer thickness; in the limit of a thick I-layer, it transforms to the AB dependence [36]. A good agreement of the theoretical and experimental dependences for sample S + 22.5Sm0 is seen in figure 6. A better coincidence is achieved for FT $I_1(T)$, and this fact was analysed in detail in [20]. We

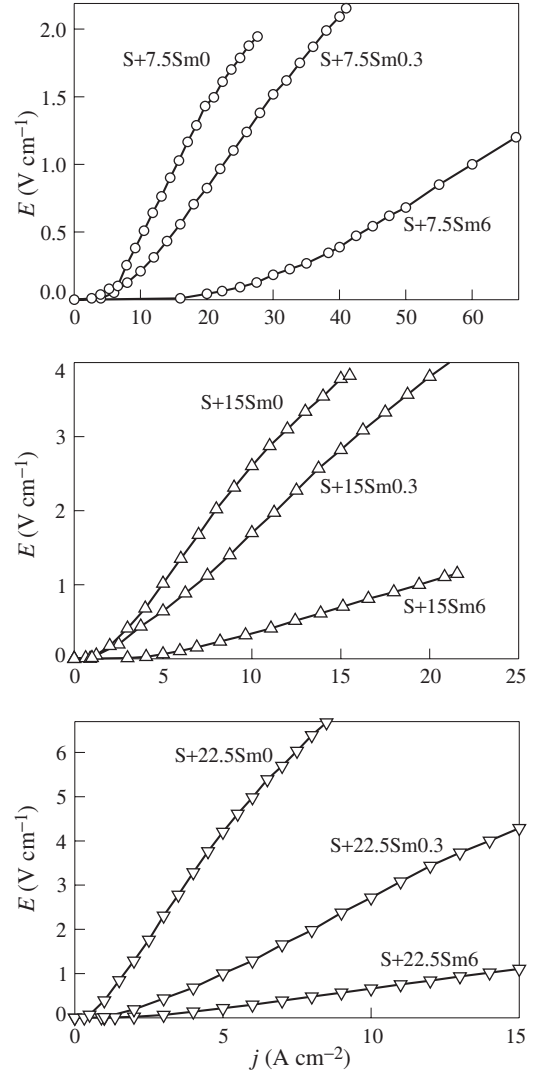


Figure 7. Experimental I – V characteristics of composite samples, measured at 4.2 K.

failed to fit satisfactorily the $R(T)$ dependence for sample S + 22.5Sm0.3 in the entire experimental temperature range with AB or FT dependences. For sample S + 22.5Sm6, this fit is even poorer. The same situation is observed for samples with 7.5 and 15 vol% semiconductor. This means that even at low carrier concentrations in the Sm-layers (sample S + 22.5Sm0.3) the TAPS approach with $I_1(T)$ for a tunnel junction becomes inapplicable. The ‘negative’ result of the fit reveals, however, a transformation of weak links in the HTSC + $\text{Cu}_{1-x}\text{Li}_x\text{O}$ composites on raising the Li content. For a correct description of the $R(T)$ dependences for S–Sm–S weak links it is necessary to use $I_1(T)$ for a S–Sm–S junction (which is presently questionable [37]) and take into account the conductivity of the Sm-layers in the TAPS mechanism.

3.5. I – V characteristics of the composites

Figure 7 shows experimental I – V characteristics of the composites, measured at 4.2 K. The I – V characteristics are characterized by the existence of a critical current (J_C) and exhibit non-linear behaviour at currents higher than J_C . For

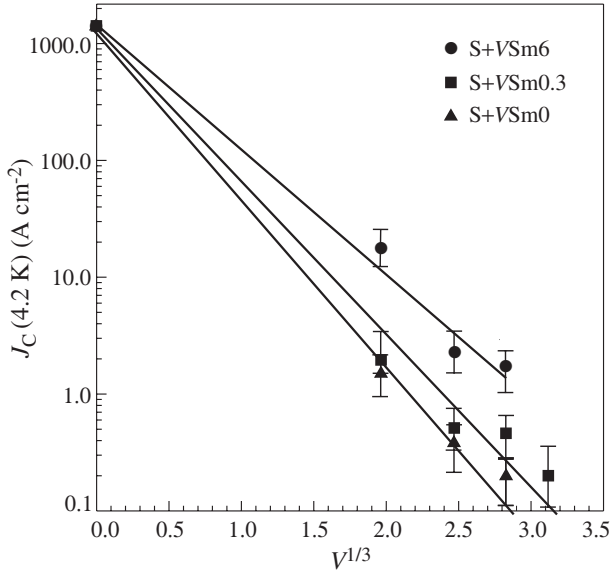


Figure 8. Critical current density at 4.2 K, $J_C(4.2 \text{ K})$, of composites $S + V\text{Sm}X$ for different X versus $V^{1/3}$ in a semi-log scale. The full curves represent approximations of the data for composite samples with the same X .

the composites with the same volume content of $\text{Cu}_{1-x}\text{Li}_x\text{O}$ the I – V characteristics are seen to change from quasi-tunnelling to quasi-metallic as the Li content, i. e. the carrier concentration in Sm-layers, increases. This result is in good agreement with a theoretical analysis of transformations of this kind in a Josephson junction [38]. A similar crossover of I – V characteristics has been observed previously in single Josephson junctions based on conventional superconductors, with light induced carriers in sensitive barriers [25, 37].

The increase in the differential resistance on raising the volume content of $\text{Cu}_{1-x}\text{Li}_x\text{O}$ (at constant x) is a manifestation of the growing effective length of semiconductor interlayers in the composites.

3.6. Temperature dependences of the critical current density of the composites

For the HTSC + normal metal composites (BaPbO_3) [13] prepared in the same manner as the composites under consideration, the experimental temperature dependences of critical current are found to be well described by the theory [39] for S–N–S junctions on the assumption that the cube root of the volume content of the non-superconducting component is proportional to the effective thickness of N-layers between HTSC crystallites in the composites. For this reason, we plot the data for $S + V\text{Sm}X$ composites as a function of $V^{1/3}$. The logarithmic plot of $J_C(4.2 \text{ K})$ versus $V^{1/3}$ is shown for the composites studied in figure 8. The data for $J_C(4.2 \text{ K}) \approx 1.4 \text{ kA cm}^{-2}$ are plotted for the bench-mark HTSC sample, see section 3.2. $J_C(4.2 \text{ K})$ values are seen to grow with increasing carrier concentration (i. e. x). The decrease in $J_C(4.2 \text{ K})$ with increasing $V^{1/3}$ can be approximated by an exponential function $\exp(-V^{1/3})$ within experimental error. An exponential decay, $\exp(-2a)$, where $2a$ is the weak link length, has been observed in experiments on single S–Sm–S junctions [40, 41] and predicted theoretically for S–Sm–S weak links [42].

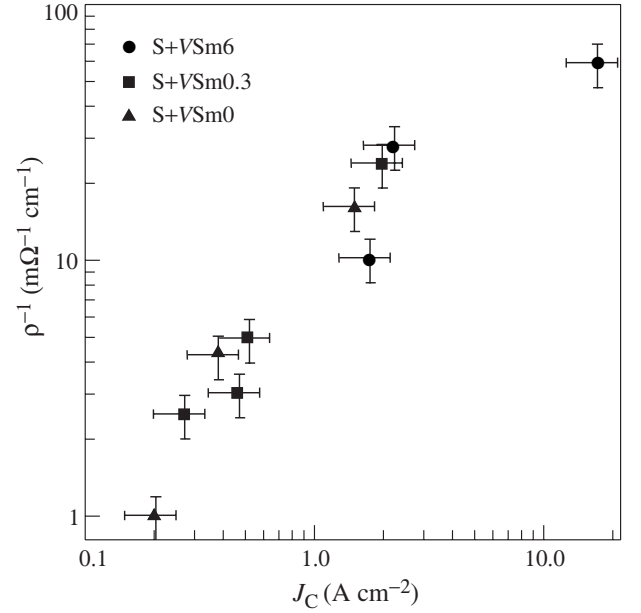


Figure 9. The log–log plot of the reciprocal of normal resistance, ρ_N^{-1} , versus critical current density J_C at 4.2 K for $S + V\text{Sm}X$ composites.

Figure 9 presents the reciprocal of the normal resistance of the composites, ρ_N^{-1} , determined from I – V characteristics (figure 7), as a function of $J_C(4.2 \text{ K})$. This dependence follows within experimental error the linear law with a slope close to unity, i. e. $J_C \sim 1/\rho_N$, a dependence characteristic of single Josephson junctions [25], is observed for the composite samples.

In figure 10 we plotted the $J_C(T)$ dependences of the composites in the co-ordinates $J_C(T)/J_C(4.2 \text{ K}) - V^{1/3} - T$. The $J_C(T)$ dependences for samples $S + V\text{Sm}0$ have the same shape as $J_C(T)$ for $S + V\text{Sm}0.3$ composites [20]. Some experimental features of the $J_C(T)$ dependences are noteworthy. The temperature at which $J_C \rightarrow 0$ ($< 10^{-4} \text{ A cm}^{-2}$) decreases with increasing $V^{1/3}$ and decreasing x . The $J_C(T)$ dependence for sample $S + 7.5\text{Sm}6$ has a feature in the low-temperature region in the form of a change in curvature. This feature was fully and repeatedly reproduced on different samples of the $S + 7.5\text{Sm}6$ set. For sample $S + 15\text{Sm}6$, this feature is less pronounced. The $J_C(T)$ for sample $S + 22.5\text{Sm}6$ has negative curvature up to 4.2 K (see inset of figure 10 for more detail).

If the change in the $J_C(T)$ curvature occurred for chemical reasons via diffusion of Li diffusion into HTSC crystallites, one would expect enhancement of the effect with increasing $\text{Cu}_{0.94}\text{Li}_{0.06}\text{O}$ volume fraction in the composites. An opposite situation, however, takes place in the experiment. Therefore, the observed behaviour is due to the occurrence of physical phenomena in S–Sm–S weak links with varying carrier concentration in Sm layers.

Several theoretical works have been devoted to critical currents in S–Sm–S junctions [42–45]. Analysis of the experimental $J_C(T)$ for HTSC+ $\text{Cu}_{1-x}\text{Li}_x\text{O}$ composites shows good qualitative agreement with the theory [42] in which the only mechanism producing the Josephson effect is the Andreev scattering. The theory [42] predicts a change in the curvature and appearance of a plateau in the $J_C(T)$ dependence near

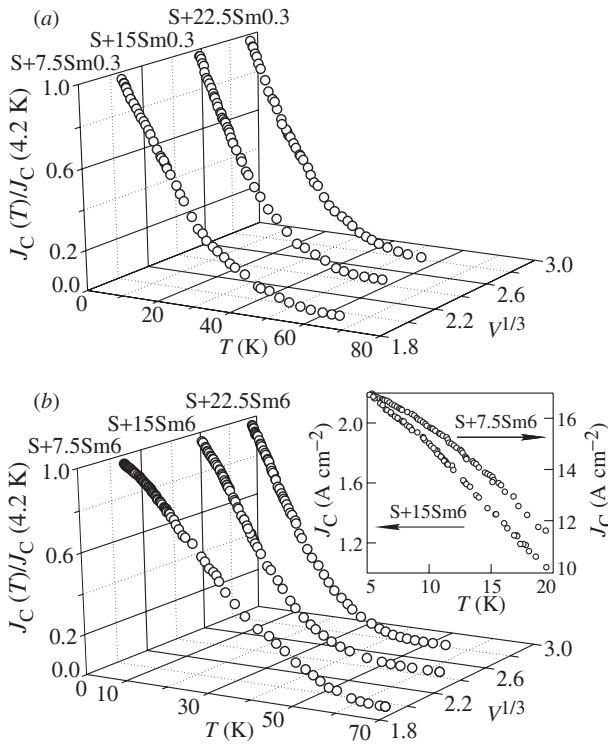


Figure 10. Normalized critical current $J_C(T)/J_C(4.2\text{ K})$ for composites (a) S + VSm0.3 and (b) S + VSm6 versus temperature and cube root of the volume concentration of $\text{Cu}_{1-x}\text{Li}_x\text{O}$. The inset shows details of $J_C(T)$ for samples S + 7.5Sm6 and S + 15Sm6 in the low-temperature region.

$T \approx 0.1T_C$ when the carrier concentration in the Sm-layer increases from 10^{16} up to $10^{17-19}\text{ cm}^{-3}$. The theory [42] also accounts for the disappearance of dissipation-free currents in the high-temperature region. The increase in the carrier concentration leads to lower zero-resistivity T_C .

The results of numerical calculations of $J_C(T)$ dependences are presented in [42] for S–Sm–S junctions with $2a = 1.57\xi_0$ (where ξ_0 is the coherence length). For the HTSC + BaPbO_3 composites [13], the effective interlayer length $2a \approx 3\xi_0$ was estimated in terms of the theory [39] for S–N–S junctions for a sample with 7.5 vol% normal metal. Unfortunately, the absence of calculated $J_C(T)$ dependences for different $2a$ values in [42] gives no way of making a correct quantitative comparison of the experiment and the theory. Nevertheless, we regard the appearance of a change in the $J_C(T)$ curvature in the low-temperature region with increasing carrier concentration in the semiconductor, not predicted by other theories [43–45], as an indirect proof of the applicability of the theory [42] to describe experimental $J_C(T)$ for the HTSC + $\text{Cu}_{1-x}\text{Li}_x\text{O}$ composites. This supports the conclusion made in [42] that the Andreev scattering in S–Sm–S junctions deserves at least as much attention as the proximity effect.

4. Conclusion

$\text{Cu}_{1-x}\text{Li}_x\text{O}$ compounds (with $x = 0, 0.003, 0.01, 0.03$ and 0.06) have been synthesized. The resistivity and magnetic measurements indicate that lithium dissolves in the CuO matrix.

Bulk $\text{Y}_{3/4}\text{Lu}_{1/4}\text{Ba}_2\text{Cu}_3\text{O}_7 + \text{Cu}_{1-x}\text{Li}_x\text{O}$ composites with $x = 0, 0.003, 0.06$ and varied volume content of $\text{Cu}_{1-x}\text{Li}_x\text{O}$ have been prepared. XRD analysis, combined with magnetic and resistive measurements, demonstrates that the superconducting properties of HTSC crystallites in the composites remain virtually unchanged, compared with those of the initial HTSC.

The obtained temperature dependences of resistivity and I – V characteristics indicate that a network of weak links exists in the composites. The monotonic change in transport properties ($\rho(T_C)$, $\rho(270\text{K})$, $J_C(4.2\text{ K})$, R_N) of the composites, and also the fact that the TAPS mechanism fails to describe $R(T)$ dependences in terms of fluctuation-free critical current for a S–I–S junction with increasing $\text{Cu}_{1-x}\text{Li}_x\text{O}$ conductivity, indicate that weak links in the composites are transformed as the x value of the semiconductor decreases. The changeover of the I – V characteristics from quasi-tunnelling to metallic-like with increasing carrier concentration in $\text{Cu}_{1-x}\text{Li}_x\text{O}$ is evidence that weak links in the composites studied are of S–Sm–S type.

The dependences of $J_C(4.2\text{ K})$ on R_N and on the effective thickness $V^{1/3}$ of weak links for the composites studied behave as single S–Sm–S junctions. The experimental temperature dependences of the critical current are qualitatively described in terms of the theory developed in [42], which takes into account the Andreev reflection as the main mechanism producing the Josephson effect in an S–Sm–S junction.

Acknowledgments

The authors wish to thank Professor R Kümmel (University of Würzburg, Germany) for his interest in the study.

References

- [1] Mannhart J, Chaudhari P, Dimos D, Tsuei C C and McGuire T R 1988 *Phys. Rev. Lett.* **61** 2476
- [2] Stephens R B 1989 *Cryogenics* **29** 399
- [3] Weinberger B R, Lynds L, Potrepka D M, Show D B, Burila C T, Eaton Jr. H E, Cipolli R, Tan Z and Budnick J I 1989 *Physica C* **161** 91
- [4] Xiao G, Stretz F H, Cieplak M Z, Bakhshai A, Garvin A and Chen C L 1988 *Phys. Rev. B* **38** 776
- [5] Calabrese J J, Dubson M A and Garland J C 1992 *J. Appl. Phys.* **72** 2958
- [6] Reich S, Veretnik D, Felner I and Yaron U 1992 *J. Appl. Phys.* **72** 4805
- [7] Jung J, Mohamed M A-K, Isaak I and Friedrich L 1994 *Phys. Rev. B* **49** 12188
- [8] Tarenkov V Yu, D'yachenko A I and Vasilenko A V 1994 *Phys. Solid State* **36** 1197
- [9] Smirnov B I and Orlova T S 1994 *Phys. Solid State* **36** 1883
- [10] Rao A S 1994 *Physica C* **235–240** 3437
- [11] Kazin P E, Polvates V V, Tretyakov Y D, Jansen M, Freitag B and Mader W 1997 *Physica C* **280** 253
- [12] Su X D, Yang Z Q, Wang Y Z, Tang H, Zhang C, Hua L and Qiao G W 1997 *Physica C* **282–287** 1615
- [13] Petrov M I, Balaev D A, Ospishchev S V, Shaihtudinov K A, Khrustalev B P and Aleksandrov K S 1997 *Phys. Lett. A* **237** 85
- [14] Petrov M I, Balaev D A, Gohfeld D M, Ospishchev S V, Shaihtudinov K A and Aleksandrov K S 1999 *Physica C* **314** 51
- [15] Masterov V F, Fyodorov A F and Chursinov A N 1992 *Sverkhprovodn., Fiz. Khim. Tekh. (USSR)* **5** 653 (in Russian)

- [16] Koshi J, Pausole K V, Jayaraj M K and Damodaran A D 1993 *Phys. Rev. B* **47** 15304
- [17] Thomas J K, Koshy J, Kurian J, Yadava Y P and Damodaran A D 1994 *J. Appl. Phys.* **76** 2376
- [18] Kim C J, Kim K-B, Kuk I-H, Hong G W 1995 *Physica C* **255** 95
- [19] Berling D, Loegel B, Mehdaoui A, Regnier S, Cananoni C and Marfaing J 1998 *Supercond. Sci. Technol.* **11** 1292
- [20] Petrov M I, Balaev D A, Shaihtudinov K A, Aleksandrov K S 1999 *Phys. Solid State* **41** 881
- [21] Koffyberg F P and Benko F A 1982 *J. Appl. Phys.* **53** 1173
- [22] Gizhevskii B A, Samokhvalov A A, Chebotaev N M, Naumov S V and Pokazan'eva G K 1991 *Sverkhprovodn., Fiz. Khim. Tekh. (USSR)* **4** 827 (in Russian)
- [23] Feduzi R, Lanza F and Dallacasa V 1993 *Mod. Phys. Lett. 7* 163
- [24] Aleksandrov K S, Vasilyev A D, Zwegintsev S A, Petrov M I and Khrustalev B P 1988 *Physica C* **156** 249
- [25] Barone A and Paterno J 1982 *Physics and Application of the Josephson Effect* (New York: Wiley)
- [26] Efros A L and Shklovskii B I 1975 *J. Phys. C: Solid State Phys.* **8** 49
- [27] Efimov A I, Belorukova L P, Vasil'kova I V and Chechev V P 1983 *Properties of Inorganic Compounds: Reference Book* (Leningrad: Himiya) (in Russian)
- [28] Carreta P, Corti M, Rigamonti A and Parmigiani F 1993 *J. Phys.: Condens. Matter.* **5** 83
- [29] Ausloos M, Laurent Ch, Vanderschueren H W, Rulmont A and Tarte P *Solid State Commun.* **68** 539
- [30] Wright A C, Zhang K and Erbil A 1991 *Phys. Rev. B* **44** 863
- [31] Gerber A, Grenet T, Cyrot M and Beille J 1991 *Phys. Rev. B* **43** 12935
- [32] Early E A, Jardim R F, Almasan C C and Maple M B 1995 *Phys. Rev. B* **51** 8560
- [33] Gross R, Chaudhari P, Dimos D, Gupta A and Koren G 1990 *Phys. Rev. Lett.* **64** 228
- [34] Ambegaokar V and Halperin B I 1969 *Phys. Rev. Lett.* **22** 1364
- [35] Ambegaokar V and Baratoff A 1963 *Phys. Rev. Lett.* **10** 486 —1963 *Phys. Rev. Lett.* **11** 104
- [36] Furusaki A and Tsukada M 1991 *Phys. Rev. B* **43** 10 164
- [37] Kleinsasser A W 1991 *IEEE Trans. Magn.* **27** 2589
- [38] Blonder G E, Tinkham M and Klapwijk T M K 1982 *Phys. Rev. B* **25** 4515
- [39] Günsenheimer U, Schussler U and Kümmel R 1994 *Phys. Rev. B* **49** 6111
- [40] Takayanagi H and Kawakami T 1985 *Phys. Rev. Lett.* **54** 2449
- [41] Gudkov A L, Kuprianov M Yu and Likharev K K 1988 *Sov. Phys. JETP* **67** 1478
- [42] Schussler U and Kümmel R 1993 *Phys. Rev. B* **47** 2754
- [43] Aslamazov L G and Fistul M V 1981 *JETP Lett.* **30** 213
- [44] Itskovich I F and Shekhter R I 1981 *Sov. J. Low. Temp. Phys.* **7** 418
- [45] Alfeev V N, Gritsenko N I 1982 *Sov. Phys. Solid State* **24** 1258